

6. V. S. Belyaev and Yu. D. Chashechkin, "Free thermoconcentration convection regimes over a localized heat source," *Izv. Akad. Nauk SSSR, Mekh. Zhidk. Gaza*, No. 2 (1989).
7. B. R. Morton, "Buoyant plumes in a moist atmosphere," *J. Fluid Mech.*, 2, Part 2 (1957).
8. A. B. Tsinober, Y. Yahalom, and D. J. Shlien, "A point source of heat in a stable salinity gradient," *J. Fluid Mech.*, 135, 199 (1983).
9. D. E. Mowbray, "The use of schlieren and shadowgraph techniques in the study of flow patterns in density stratified liquids," *J. Fluid Mech.*, 27, Part 2 (1967).
10. S. N. Netreba, "Reaction of stratified rotating media to local thermal effects," *Prikl. Mat. Mekh.*, 50, No. 5 (1986).
11. A. S. Kabanov and S. N. Netreba, "Free convection from a point heat source in a stably stratified medium," *Prikl. Mat. Mekh.*, 46, No. 1 (1982).
12. *Oceanology, Physics of the Ocean, Vol. 2: Ocean Hydrodynamics* [in Russian], Nauka, Moscow (1978).
13. G. K. Batchelor, *An Introduction to Fluid Dynamics*, Cambridge Univ. Press (1973).
14. F. Olver, *Introduction to Asymptotics and Special Functions*, Academic Press, New York (1974).
15. L. N. Sretenskii, *Theory of Fluid Wave Motions* [in Russian], Nauka, Moscow (1977).

PROPAGATION OF PLANE SURFACE WAVES OVER AN UNDERWATER OBSTACLE  
AND A SUBMERGED PLATE

I. V. Sturova

UDC 532.59

The investigation, in the linear formulation, of wave diffraction by bottom irregularities with shadow zones, begun in [1], is continued. A rectangular underwater obstacle with a "lid" and a rigidly clamped horizontal plate (Fig. 1) are considered.

Wave scattering by an ordinary rectangular obstacle (without a "lid") has been studied in detail, both theoretically [2-5] and experimentally [6]. In [5] it is assumed that away from the obstacle the fluid is infinitely deep. Wave scattering by a horizontal plate on a free surface was examined in [3, 7].

1. Waves are propagated in a layer of ideal incompressible liquid of depth  $H_1$ , on the bottom of which lies a rectangular obstacle with a "lid" in the form of an infinitely thin rigid horizontal plate (Fig. 1a). This plate is located at a depth  $H_2$  below the free surface. The length of the plate  $L$  may be greater than the base of the obstacle  $AB$ , so that on the left and right of the obstacle there are cavities of length  $\ell_1$  and  $\ell_2$ , respectively. The coordinate system is so chosen that the  $x$  axis coincides with the undisturbed level of the free surface, and the  $y$  axis is directed upwards through the left-hand end of the lid. The motion of the fluid is assumed to be potential everywhere except at the corner points.

The approaching wave travels in the direction of the positive  $x$  axis and is determined by the velocity potential  $\Phi_0(x, y, t) = \varphi_0(x, y) \exp(-i\sigma t)$ , where  $\varphi_0 = \frac{ia g \operatorname{ch} k_1(y + H_1)}{\sigma \operatorname{ch} k_1 H_1} \exp(ik_1 x)$ ;  $a$  and  $\sigma$  are the amplitude and frequency of the wave, and  $g$  is the acceleration of gravity; the wave number  $k_1$  is determined from the equation

$$\sigma^2 = g k_1 \operatorname{th} k_1 H_1. \quad (1.1)$$

Here and in what follows in all the expressions containing the factor  $\exp(-i\sigma t)$  only the real part has physical significance.

We will consider steady waves and seek the velocity potential of the disturbed flow in the form  $\Phi(x, y, t) = \varphi(x, y) \exp(-i\sigma t)$ . In order to determine  $\varphi(x, y)$  we must solve the

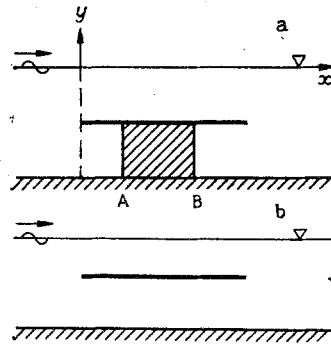


Fig. 1

problem

$$\Delta\varphi = 0 \quad (x, y \in S), \quad (1.2)$$

$$\sigma^2\varphi - g\partial\varphi/\partial y = 0 \quad (y = 0), \quad \partial\varphi/\partial n = 0 \quad (\text{on the solid boundaries}),$$

where  $S$  is the domain occupied by the fluid, and  $n$  is the normal to the bottom. The reflected and transmitted waves must satisfy the radiation conditions as  $|x| \rightarrow \infty$ .

For solving the problem (1.2) we will use a matching method similar to that used in [1, 2]. The domain  $S$  is divided into five rectangular parts:

$$\begin{aligned} S_1 &= [-\infty < x < 0, -H_1 \leq y \leq 0], \\ S_2 &= [0 < x < L, -H_2 \leq y \leq 0], \\ S_3 &= [L < x < \infty, -H_1 \leq y \leq 0], \\ S_4 &= [0 < x < l_1, -H_1 \leq y \leq -H_2], \\ S_5 &= [L - l_2 < x < L, -H_1 \leq y \leq -H_2], \end{aligned} \quad (1.3)$$

in each of which  $\varphi(x, y)$  is denoted by  $\varphi_j(x, y)$  ( $j = 1, \dots, 5$ ). We will seek the functions  $\varphi_j$  in the form of an expansion in the eigenfunctions of the corresponding boundary value problems:

$$\begin{aligned} \varphi_1 &= \varphi_0 + A_0 \exp(-ik_1x) Y_1(y) + \sum_{n=1}^{\infty} A_n \exp(k_{1n}x) Y_{1n}(y), \\ \varphi_2 &= [B_0 \exp(ik_2x) + C_0 \exp(-ik_2x)] Y_2(y) + \\ &+ \sum_{n=1}^{\infty} [B_n \exp(k_{2n}x) + C_n \exp(-k_{2n}x)] Y_{2n}(y), \\ \varphi_3 &= D_0 \exp(ik_1x) Y_1(y) + \sum_{n=1}^{\infty} D_n \exp(-k_{1n}x) Y_{1n}(y), \\ \varphi_4 &= \alpha_0 + \sum_{m=1}^{\infty} \alpha_m \operatorname{ch} \beta_m(l_1 - x) \cos \beta_m(y + H_1), \\ \varphi_5 &= \gamma_0 + \sum_{m=1}^{\infty} \gamma_m \operatorname{ch} \beta_m(x - L + l_2) \cos \beta_m(y + H_1). \end{aligned} \quad (1.4)$$

Here  $\beta_m = \pi m/h$ ;  $h = H_1 - H_2$ ; and  $k_{1n}$  ( $n = 1, 2, \dots$ ) are the roots of the equation

$$\sigma^2 = -gk \operatorname{tg} k H_1. \quad (1.5)$$

The quantities  $k_2$  and  $k_{2n}$  are determined from the Eqs. (1.1) and (1.5) with  $H_1$  replaced by  $H_2$ . The eigenfunctions  $Y_i, Y_{in}$  ( $i = 1, 2$ ) are orthogonal and normalized as follows:

$$Y_i(y) = \frac{\operatorname{ch} k_i(y + H_i)}{\sqrt{\Lambda_i}}, \quad \Lambda_i = \int_{-H_i}^0 \operatorname{ch}^2 k_i(y + H_i) dy.$$

$$Y_{in}(y) = \frac{\cos k_{in}(y + H_i)}{\sqrt{\Lambda_{in}}}, \quad \Lambda_{in} = \int_{-H_i}^0 \cos^2 k_{in}(y + H_i) dy.$$

Because of the continuity of the motion in the domain S on the boundary of the domains  $S_j$ , pressure and horizontal velocity matching conditions are imposed, from which it follows that: when  $x = 0$

$$\begin{aligned} \varphi_1 &= \varphi_2, \quad \partial\varphi_1/\partial x = \partial\varphi_2/\partial x \quad (-H_2 \leq y \leq 0), \\ \varphi_1 &= \varphi_4, \quad \partial\varphi_1/\partial x = \partial\varphi_4/\partial x \quad (-H_1 \leq y \leq -H_2), \end{aligned}$$

and when  $x = L$

$$\begin{aligned} \varphi_2 &= \varphi_3, \quad \partial\varphi_2/\partial x = \partial\varphi_3/\partial x \quad (-H_2 \leq y \leq 0), \\ \varphi_3 &= \varphi_5, \quad \partial\varphi_3/\partial x = \partial\varphi_5/\partial x \quad (-H_1 \leq y \leq -H_2). \end{aligned}$$

Using the reduction method, we replace the infinite series in (1.4) by finite sums with N and M terms, respectively. The matching conditions (1.6) are integrally satisfied, i.e., they are successively multiplied by the eigenfunctions  $Y_{i1}$ ,  $Y_{in}$  ( $n = 1, \dots, N$ ), and  $\cos \beta_m(y + H_1)$  ( $m = 1, \dots, M$ ) and integrated over the interval  $-H_1 \leq y \leq 0$  (for further details see [1]). The constants  $\alpha_m$  and  $\gamma_m$  may conveniently be expressed in terms of the remaining unknown complex constants, and the problem finally reduces to the numerical solution of a system of  $4 + 4N$  linear equations.

2. Wave propagation in the presence of a submerged horizontal plate (Fig. 1b) differs from the case of a rectangular obstacle mainly in that the fluid is able to flow beneath the plate. In order to solve this problem we divide the flow domain S into four rectangular parts, of which  $S_1$ ,  $S_2$ , and  $S_3$  coincide with those introduced in (1.3), while  $S_4 = [0 < x < L, -H_1 \leq y \leq -H_2]$ . The function  $\varphi_4$  is found in the expanded form:

$$\varphi_4 = \alpha_0 + bx + \sum_{m=1}^{\infty} (\alpha_m \operatorname{sh} \beta_m x + \gamma_m \operatorname{ch} \beta_m x) \cos \beta_m (y + H_1). \quad (2.1)$$

The functions  $\varphi_1$ ,  $\varphi_2$ ,  $\varphi_3$  coincide with (1.4). A particular case of this problem is that of a plate on the free surface ( $H_2 = 0$ ). Then the flow domain can be divided into parts  $S_1$ ,  $S_3$ , and  $S_4$ , in which the solution is represented by expressions (1.4) for  $\varphi_1$  and  $\varphi_3$  and (2.1) for  $\varphi_4$  with  $\beta_m = m\pi/H_1$ . The method of solution is similar to that of Sec. 1 and the problem reduces to a system of  $4 + 4N$  linear equations for a submerged and  $2 + 2N$  equations for a floating plate.

The approximation in which the infinite sums in (1.4) and (2.1) are not taken into account is often used for investigating wave diffraction by rectangular obstacles. The problem is then easy to solve analytically and, in particular, for the characteristics of the reflected and transmitted waves we have the expressions

$$A_0^* = i\Gamma [2QZ(1 - \cos \theta) - (1 - Z^2)\sin \theta], \quad D_0^* = 2\Gamma(Q \sin \theta + Z), \quad (2.2)$$

$$\text{where } (A_0^*, D_0^*) = \frac{\sigma \operatorname{ch} k_1 H_1}{ag \sqrt{H_1 \Lambda_1}} (A_0, \exp(ik_1 L) D_0),$$

$$\begin{aligned} \Gamma &= \sin \theta [i \sin \theta + Z(1 - \cos \theta)]^{-1} [\sin \theta (i - 2Q) - Z(1 + \cos \theta)]^{-1}, \\ \theta &= k_2 L, \quad Q = \frac{\operatorname{sh}^2 k_1 h}{L h k_1^3 \Lambda_1}, \quad Z = \frac{k_1 k_2 \operatorname{sh}^2 k_1 h}{\Lambda_1 \Lambda_2 (k_2^2 - k_1^2)}. \end{aligned}$$

The reflection and transmission coefficients R and T are determined as follows:

$$(R, T) = \frac{\sigma \operatorname{ch} k_1 H_1}{ag \sqrt{\Lambda_1}} (|A_0|, |D_0|) = (|A_0^*|, |D_0^*|).$$

In this approximation the horizontal flow velocity beneath the plate

$$b^* = \frac{\sigma b H_1}{ag} = \frac{H_1 \operatorname{sh} k_1 h}{k_1 L h \operatorname{ch} k_1 H_1} (D_0^* - A_0^* - i). \quad (2.3)$$

In the long-wave approximation ( $k_1 H_1, k_2 H_2 \rightarrow 0$ ) in expressions (2.2) we must use

$$Q = \frac{h}{L k_2 \sqrt{H_1 H_2}}, \quad Z = \sqrt{\frac{H_2}{H_1}}, \quad k_2 = \frac{\sigma}{\sqrt{g H_2}}. \quad (2.4)$$

For a floating plate expressions (2.2) can be considerably simplified:  $A_0^* = \frac{1}{2Q - i}$ ,  $D_0^* = \frac{2iQ}{2Q - i}$ ,

and the reflection and transmission coefficients and the modulus of the horizontal velocity take the form:

$$R = \frac{1}{\sqrt{4Q^2 + 1}}, \quad T = \frac{2Q}{\sqrt{4Q^2 + 1}}, \quad |b^*| = \frac{2 \operatorname{th} k_1 H_1}{k_1 L \sqrt{4Q^2 + 1}}. \quad (2.5)$$

In the long-wave approximation these expressions give the well-known relations [7]:

$$R = \frac{c}{\sqrt{4 + c^2}}, \quad T = \frac{2}{\sqrt{4 + c^2}}, \quad |b^*| = \frac{2cH_1}{L \sqrt{4 + c^2}} \quad (c = \sigma L / \sqrt{g H_1}). \quad (2.6)$$

From relations (2.2) it is also easy to obtain the results of this approximation in the case of a rectangular obstacle; in this case the water cavities  $S_4$  and  $S_5$  are unimportant. For a rectangular obstacle we must set  $Q \equiv 0$ ; then  $A_0^* = i(1 - Z^2)/d$ ,  $D_0^* = -2Z/d \sin \theta$  ( $d = 1 + Z^2 + 2iZ/\tan \theta$ ). The reflection and transmission coefficients take the form:

$$R = f(1 - Z^2) \sin \theta, \quad T = 2fZ \quad (f = [4Z^2 + (1 - Z^2) \sin^2 \theta]^{-1/2}). \quad (2.7)$$

In order to obtain the long-wave approximation it is necessary to take the representation (2.4) for  $Z$  in (2.7). We note that the two approximate solutions obtained for a rectangular obstacle are identical to the results given in [1] for a trench.

3. In the numerical calculations we determined the reflection and transmission coefficients, the constant component of the horizontal velocity for the plate, and the kinetic energy of the fluid enclosed in the cavities. In the case of a rectangular obstacle the kinetic energies  $E_{k1}$  and  $E_{k2}$  in the domains  $S_4$  and  $S_5$ , respectively, averaged over the oscillation period and divided by the length  $h$ , are written as follows:

$$E_{k1} = -\frac{\rho}{2h} \left\langle \int_{-H_1}^{-H_2} \Phi_4 \frac{\partial \Phi_4}{\partial x} dy \right\rangle = \frac{\rho}{16} \sum_{m=1}^{\infty} \beta_m |\alpha_m|^2 \operatorname{sh} 2\beta_m l_1; \quad (3.1)$$

$$E_{k2} = \frac{\rho}{2h} \left\langle \int_{-H_1}^{-H_2} \Phi_5 \frac{\partial \Phi_5}{\partial x} dy \right\rangle = \frac{\rho}{16} \sum_{m=1}^{\infty} \beta_m |\gamma_m|^2 \operatorname{sh} 2\beta_m l_2, \quad (3.2)$$

where  $\rho$  is the density of the fluid, and  $\langle \rangle$  denotes averaging with respect to time; the integration is carried out at  $x = 0$  for  $E_{k1}$  and  $x = L$  for  $E_{k2}$ . The ratio of these quantities to the energy of the approaching wave per unit length  $E_b = \rho g a^2 / 4$  is equal to  $E_i = E_{ki} / E_b$  ( $i = 1, 2$ ).

In the case of a submerged plate by analogy with (3.1)

$$E_{k1} = -\frac{\rho}{8} \left( 2\xi_0 + \sum_{m=1}^{\infty} \xi_m \beta_m \right), \quad (3.3)$$

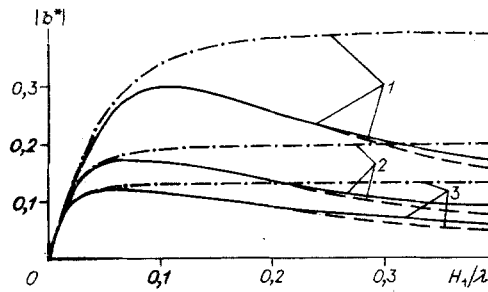


Fig. 2

TABLE 1

N; M	$H_1/\lambda$											
	0,05			0,1			0,15			0,2		
	R·10	$E_1 \cdot 10^2$	$E_2 \cdot 10$	R·10	$E_1 \cdot 10^2$	$E_2 \cdot 10^2$	R·10	$E_1 \cdot 10^2$	$E_2 \cdot 10^2$	R·10	$E_1 \cdot 10^2$	$E_2 \cdot 10^2$
7: 40	4,065	8,05	1,105	5,159	3,84	8,24	4,258	4,06	7,31	1,063	6,16	6,75
7: 80	4,064	8,06	1,106	5,159	3,84	8,25	4,257	4,06	7,32	1,062	6,17	6,76
10: 40	4,089	7,22	1,001	5,188	3,38	7,47	4,308	3,56	6,63	1,152	5,54	6,15
15: 40	4,109	6,96	0,969	5,213	3,23	7,21	4,352	3,39	6,39	1,232	5,31	5,95
20: 40	4,119	6,79	0,947	5,225	3,13	7,05	4,373	3,28	6,24	1,272	5,16	5,82
20: 80	4,118	6,82	0,952	5,224	3,15	7,08	4,372	3,30	6,27	1,269	5,19	5,85

and in (3.2)  $\Phi_5$  must be replaced by  $\Phi_4$ :

$$E_{k2} = \frac{\rho}{16} \left\{ 4(L|b|^2 + \xi_0) + \sum_{m=1}^{\infty} \beta_m (|\alpha_m|^2 + |\gamma_m|^2) \operatorname{sh} 2\beta_m L + 2\xi_m \operatorname{ch} 2\beta_m L \right\}. \quad (3.4)$$

Here  $\xi_0 = \alpha_0^r b^r + \alpha_0^i b^i$ ;  $\xi_m = \alpha_m^r \gamma_m^r + \alpha_m^i \gamma_m^i$ ; the superscripts r and i denote the real and imaginary parts.

The convergence of the numerical results as a function of the number of terms retained in the expressions (1.4) and (2.1) is given in Tables 1 and 2 for a rectangular obstacle and a plate, respectively. The value of the reflection coefficient R, the modulus of the velocity  $|b^*|$  and the energies  $E_1$  and  $E_2$  were obtained for  $H_2/H_1 = 0.2$ ,  $L/H_1 = 5$ ,  $\ell_1/H_1 = 1$ ,  $\ell_2/H_1 = 4$ , and various values of N and M as a function of the ratio  $H_1/\lambda$ , where  $\lambda = 2\pi/k_1$  is the length of the incident wave. Clearly, a change in M has almost no effect on the results, whereas varying N can have a marked effect, especially on the energy characteristics. However, for practical purposes a value  $N = 10-15$  is sufficient.

In [3] it is noted that for a plate floating at the free surface over the entire wave number interval the reflection coefficient in the complete solution is in fairly good agreement with the long-wave approximation (2.6) even when  $L/H_1 \geq 2$ . We were able to confirm this conclusion. On the interval in question for the reflection coefficient the complete solution coincides with the approximations (2.5), (2.6); however, a considerable discrepancy is observed on the short-wave interval for the value of the horizontal velocity. Figure 2 shows the function  $|b^*|$  for  $L/H_1 = 5, 10$ , and 15 (curves 1-3). The continuous curves correspond to the numerical solution with  $N = 10$ ,  $M = 40$ , the broken curves to the approximation (2.5), and the chain curves to the approximation (2.6). In the long-wave approximation (2.6) the modulus of the horizontal velocity tends to a constant value as the length of the incident wave decreases, whereas in the approximation (2.5) and the numerical solution a decrease in velocity is observed.

Figure 3 gives the values of R and  $|b^*|$  for a submerged plate (Fig. 3a, b) and R for a rectangular obstacle (Fig. 3c) when  $H_2/H_1 = 0.2$ ,  $L/H_1 = 5$ ,  $\ell_1 = \ell_2 = 0$ ,  $N = 15$ , and  $M = 40$ . The curves are distinguished in the same way as in Fig. 2. An interesting feature of the behavior of these curves is their nonmonotonic dependence on the length of the approaching wave and the fact that, although the locations of the transmission windows almost coincide (except for the first value), the local maxima of the reflection coefficient differ in the case of a rectangular obstacle and a plate. For a plate with the given initial parameters when  $H_1/\lambda \approx 0.06$  almost total reflection is observed, while for a rectangular obstacle the maximum

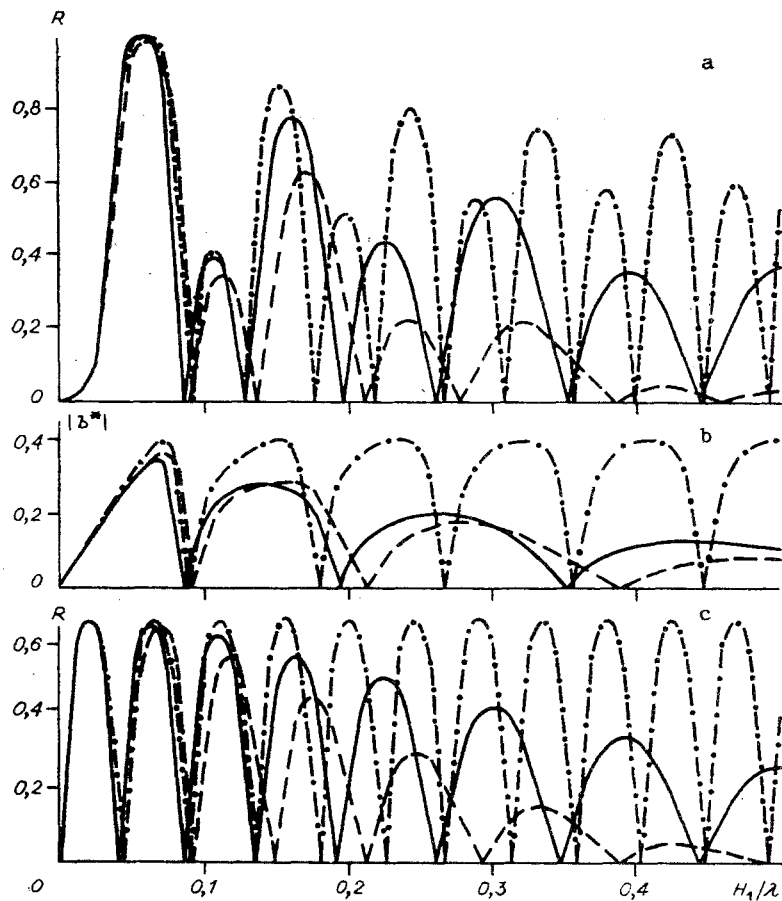


Fig. 3

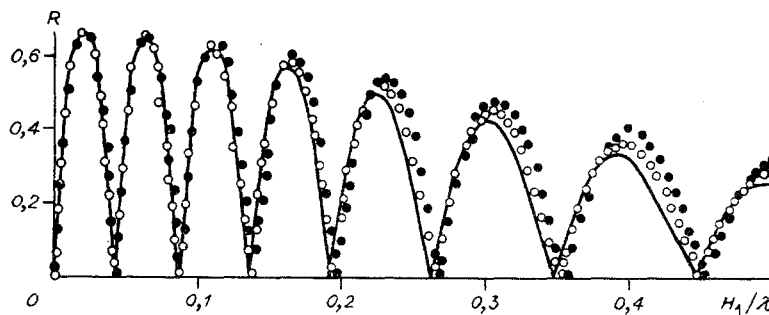


Fig. 4

value of  $R$  is only 0.66 and corresponds to  $H_1/\lambda \approx 0.02$ . We note that in the case of a rectangular obstacle and a trench (see, for example, [1]) the qualitative behavior of the reflection and transmission coefficients is the same. In both cases for the complete solution the local maxima of  $R$  decrease monotonically (and hence the local minima of  $T$  increase) as the length of the approaching wave decreases, whereas the long-wave approximation gives constant values, and the approximation (2.7), although it reflects the decrease in  $R$ , makes it more intense than in the numerical solution. In the case of a submerged plate the decrease in the local  $R$  maxima is nonmonotonic, as can also be observed in both approximations. The horizontal velocity of the flow beneath the plate also oscillates but with twice the period of the reflection coefficient, the difference between the numerical solution and the approximation (2.3) being less perceptible than for the reflection coefficient. As in the case of a trench, the approximation (2.2) gives fairly accurate results only for relatively small differences in the depths  $H_1$  and  $H_2$ .

In Fig. 4 we have plotted the reflection coefficients for a rectangular obstacle with different water cavity dimensions and the same values of the other parameters as in Fig. 3c:

TABLE 2

N; M	$H_1/\lambda$															
	0,05				0,1				0,15				0,2			
	R·10	b* ·10	E <sub>1</sub>	E <sub>2</sub> ·10	R·10	b* ·10	E <sub>1</sub> ·10	E <sub>2</sub> ·10	R·10	b* ·10	E <sub>1</sub> ·10	E <sub>2</sub> ·10	R·10	b* ·10 <sup>2</sup>	E <sub>1</sub> ·10 <sup>2</sup>	E <sub>2</sub> ·10 <sup>2</sup>
7; 40	9,442	2,800	3,4682	8,447	3,629	1,778	4,074	1,119	6,821	2,835	4,420	2,616	1,023	3,49	6,17	6,27
7; 80	9,442	2,800	3,4681	8,449	3,629	1,778	4,074	1,119	6,821	2,835	4,420	2,617	1,022	3,48	6,17	6,27
10; 40	9,450	2,800	3,4725	8,192	3,644	1,786	4,083	1,085	6,858	2,834	4,401	2,506	1,104	3,76	5,64	5,69
15; 40	9,457	2,800	3,4786	8,060	3,656	1,793	4,103	1,078	6,889	2,832	4,403	2,455	1,177	4,01	5,48	5,48
20; 40	9,460	2,800	3,4814	7,986	3,662	1,797	4,112	1,072	6,905	2,831	4,403	2,425	1,214	4,14	5,38	5,35
20; 80	9,460	2,800	3,4813	7,997	3,662	1,796	4,112	1,074	6,904	2,831	4,404	2,430	1,210	4,12	5,40	5,38

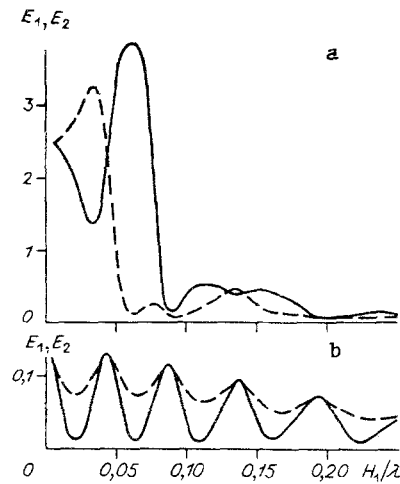


Fig. 5

1)  $\ell_1 = 5H_1$ ,  $\ell_2 = 0$  (white circles), 2)  $\ell_1 = \ell_2 = 2.5H_1$  (black circles). We note that the variant  $\ell_1 = 0$ ,  $\ell_2 = 5H_1$  almost coincided with case 1 and the variant  $\ell_1 = \ell_2 = H_1$  with 2. The curve corresponds to the variant  $\ell_1 = \ell_2 = 0$ . The effect of the cavities on the diffraction characteristics is weak and for relatively long waves almost nonexistent. As the depth of the obstacle increases, the influence of the cavities decreases. The behavior of the dynamic pressure in the cavity of an obstacle similar in shape to case 1 was investigated in [8]. It was shown that the pressure varies only at the inlet to the cavity.

The behavior of the kinetic energy (3.1)-(3.4) for a plate and a rectangular obstacle is illustrated in Figs. 5a and 5b for  $H_2/H_1 = 0.2$ ,  $L/H_1 = 5$ , and  $\ell_1 = \ell_2 = 2.5H_1$ . The continuous curve represents the values of  $E_1$ , the broken curve those of  $E_2$ . The sharp increase in  $E_1$  for a plate (Fig. 5a) when  $H_1/\lambda \approx 0.06$  corresponds to the total reflection regime for the incident wave in question. As the depth of the plate increases, this effect disappears and the energy characteristics decrease considerably. In the cavities of the obstacle the values of the kinetic energy are much smaller, and the local maxima of  $E_1$  and  $E_2$  correspond to the transmission windows in the same way as in wave propagation over a trench [1]. We note that values of  $E_1$  and  $E_2$  very similar to those presented in Fig. 5b are observed when  $\ell_1 = \ell_2 = H_1$  and, moreover, similar values of  $E_1$  when  $\ell_1 = 5H_1$ ,  $\ell_2 = 0$  and of  $E_2$  when  $\ell_1 = 0$ ,  $\ell_2 = 5H_1$ .

Our investigations of wave scattering by various rectangular obstacles confirm the wide possibilities of varying the characteristics of the reflected and transmitted waves by varying the geometry of the obstacle.

#### LITERATURE CITED

1. I. V. Sturova, "Propagation of plane surface waves over a partially covered rectangular trench," *Zh. Prikl. Mekh. Tekh. Fiz.*, No. 5 (1991).
2. K. Takano, "The effects of a rectangular obstacle on wave propagation," *Houille Blanche*, No. 3 (1960).
3. C. C. Mei and J. L. Black, "Scattering of surface waves by rectangular obstacles in waters of finite depth," *J. Fluid Mech.*, **38**, Part 3 (1969).
4. J. N. Newman, "Propagation of water waves past long two-dimensional obstacles," *J. Fluid Mech.*, **23**, Part 1 (1965).
5. S. S. Voit, "Passage of plane waves through a shallow-water zone," *Tr. Mor. Gidrofiz. Inst. Akad. Nauk SSSR*, **15** (1959).
6. G. E. Kononkova, L. M. Voronin, and K. V. Pokazeev, "Reflection of long waves by underwater obstacles," in Collection: *Theoretical and Experimental Investigation of Long-Wave Processes* [in Russian], DVNTs Akad. Nauk SSSR, Vladivostok (1985).
7. J. J. Stoker, *Water Waves*, Wiley (Interscience), New York (1957).
8. S. Massel, "O pewnym dwuwymiarowym zagadnieniu dyfrakcyjnym dla fal powierzchniowych," *Rozpr. Hydrotechn.*, No. 48 (1986).